Published in final edited form as:
Bioorg Med Chem Lett. 2010 January 15; 20(2): 665. doi:10.1016/j.bmcl.2009.11.056.

Design, synthesis and prostate cancer cell-based studies of analogs of the Rho/MKL1 transcriptional pathway inhibitor, CCG-1423

Chris R. Evelyn[a], **Jessica L. Bell**[b], **Jenny G. Ryu**[b], **Susan M. Wade**[a], **Andrew Kocab**[a], **Nicole L. Harzdorf**[b], **H. D. Hollis Showalter**[b], **Richard R. Neubig**[a,*], and **Scott D. Larsen**[b,*]

[a]Department of Pharmacology-University of Michigan Medical School, University of Michigan, Ann Arbor, MI 48109, USA

[b]Department of Medicinal Chemistry-College of Pharmacy, University of Michigan, Ann Arbor, MI 48109, USA

Abstract

We recently identified bis(amide) CCG-1423 (**1**) as a novel inhibitor of RhoA/C-mediated gene transcription that is capable of inhibiting invasion of PC-3 prostate cancer cells in a Matrigel model of metastasis. An initial structure-activity relationship study focusing on bioisosteric replacement of the amides and conformational restriction identified two compounds, **4g** and **8**, with improved selectivity for inhibition of RhoA/C-mediated gene transcription and attenuated cytotoxcity relative to **1**. Both compounds were also capable of inhibiting cell invasion with equal efficacy to **1** but with less attendant cytotoxicity.

Cancer metastasis is a tremendous medical problem responsible for thousands of deaths every year.[1] Metastases arise when dysregulation of one or more cellular processes allow malignant cells to escape the confines of the tissue of origin and establish themselves in alternate sites. Signaling through RhoA/C is important for invasion and metastasis of many cancers.[2–4] In addition to the well-known role of RhoA/C in cytoskeletal function, there is a less well understood downstream action on gene transcription.[5,6] The pathway involved in this has recently been elucidated and several components are related to cancer pathogenesis. The mitogenic G protein coupled receptor ligands bombesin, thrombin, and lysophosphatidic acid (LPA) and their receptors are well-known mitogens and stimulate tumor invasion. The novel $G\alpha_{12}$ family of heterotrimeric G proteins (G_{12} and G_{13}) activates RhoA and RhoC through guanine exchange factors such as leukemia-associated RhoGEF (LARG). Most relevant to the present work on Rho-transcriptional mechanisms are the megakaryoblastic leukemia transcriptional co-activator proteins (MKL1 & 2) which cooperate with the transcription factor, serum response factor (SRF), to increase expression of a number of genes potentially related to cancer progression and metastasis.[5,6] Exciting recent knockout and siRNA data have shown a key *in vivo* role for RhoC in breast cancer metastasis[7] and for MKL1 and SRF in melanoma and breast cancer metastases[8]. These studies provide important support for the idea that Rho

*Corresponding authors. Tel (SDL): 734 323 1187; (RRN): 734 764 8165; sdlarsen@umich.edu; rneubig@umich.edu.

NIH-PA Author Manuscript

NIH-PA Author Manuscript

signaling *and specifically Rho-regulated gene transcription* may be exciting targets for cancer therapy.

We recently identified a compound CCG-1423 (**1**) that blocks SRE-Luciferase gene transcription in response to activation of RhoA and RhoC signaling pathways.[9] Consistent with its role as a Rho/SRF pathway inhibitor, **1** potently (<1 μM) inhibited LPA-induced DNA synthesis in PC-3 prostate cancer cells. It also inhibited the growth of RhoC-overexpressing melanoma lines (A375M2 and SK-Mel-147) at nanomolar concentrations, but was less active on related cell lines (A375 and SK-Mel-28) that express lower levels of RhoC. **1** inhibited Rho-dependent invasion by PC-3 prostate cancer cells, whereas it did not affect the $G\alpha_i$-dependent invasion by the SKOV-3 ovarian cancer cell line. Thus, based on its profile, **1** is a promising lead compound for the development of novel pharmacologic tools to disrupt transcriptional responses of the Rho pathway in cancer.

Despite its favorable effects on cancer cell function, **1** did exhibit some modest acute cellular toxicity toward PC-3 cells at 24 hours as evidenced by some non-specific inhibition of gene expression (TK-*Renilla*) and a parallel decrease in a WST-1 cell viability readout. Consequently, we undertook initial molecular modifications of **1** with the goal of improving its potency and/or selectivity and attenuating its cytotoxicity. Three structural features of the lead were identified as potential areas of concern. First, the N-O bond in the tether between the two carboxamides is susceptible to reductive cleavage by thiols, thereby giving **1** the potential to non-selectively modify cysteine-containing proteins or to be cleaved by glutathione. Second, the two carboxamides could be expected to limit potency by impeding cell penetration.[10,11] Finally, the relatively flexible nature of the tether between the two aromatic rings is likely not optimal for achieving both potency and selectivity.[12] Our initial strategy to modify **1** thus included: removal of the N-O bond, bioisosteric replacement of the amides[13], and conformational restriction[14] of the tether between the aromatic rings. A limited survey of aromatic substitution was also undertaken to clarify the role of the lipophilic substituents.

The synthetic routes to new analogs of **1** are presented in Scheme 1 – Scheme 6. A preparation of bis(amides) **4** that was general for a variety of amino acids **2** (acyclic or cyclic, Table 1 and Table 4) is summarized in Scheme 1. Acylation with bis(trifluoromethyl)benzoyl chloride, either under Schotten-Baumann conditions or under anhydrous conditions, afforded the mono (amides) **3** in good yields. Final amidation with 4-chloroaniline was then effected with N-(3-dimethylaminopropyl)-N'-ethylcarbodiimide hydrochloride (EDC) and 1-hydroxybenzotriazole (HOBt) to afford bis(amides) **4**. N-methylanilide **4e**, benzylamide **4f**, and indoline amide **4p** were made under similar conditions using N-methyl-4-chloroaniline, 4-chlorobenzylamine or 5-chloroindoline, respectively, in the final amidation step. Applying the same chemistry, bis(amides) **5a–g** of aminoxyacetic acid (Table 2) with various aromatic substitution patterns were also prepared. Monoamine **8** was prepared by alkylation of 4-chloroaniline with 3-bromopropylamine **6**[15], followed by acylation with bis(trifluoromethyl) benzoyl chloride (Scheme 2). The regioisomeric monoamine **11** was synthesized by alkylation of bis(trifluoromethyl)benzylamine with bromide **10**, which was prepared by acylation of 4-chloroaniline with 3-bromopropionyl chloride (Scheme 3). Bis(amine) **12** (Table 3) could be obtained by exhaustive reduction of bis(amide) **4a** (Table 1) with borane-THF complex at reflux.

Thiazole **13** and ether **14** (Table 5) could be made by simple acylation of the respective commercially available amines with bis(trifluoromethyl)benzoyl chloride. Conformationally restricted lactam **19** required a multi-step synthesis (Scheme 4). Deprotection of commercially available N-(Boc)-4-piperidinone **15**, followed by acylation, afforded benzamide **16**. Oxime formation followed by Beckman rearrangement generated the ring-expanded intermediate diazepanone **18**. Final N-arylation of the lactam with 4-iodo-chlorobenzene under Buchwald conditions[16] then completed the synthesis. Amide **16** could also be reductively aminated with 4-chloroaniline and sodium cyanoborohydride to provide conformationally restricted amine **20** (Table 4).

Isoxazoline **23** was prepared by a cycloaddition of the nitrile-oxide derived from oxime **22**[17] with N-(4-chlorophenyl)but-3-enamide[18] (Scheme 5). Triazoles **29** and **31** were prepared from anilines **28** and **30**, respectively, by azidation and copper-catalyzed Click cyclization with alkyne amides **25** and **27** (Scheme 6).[19]

Effects on Rho-mediated gene expression, non-specific gene expression, and cytotoxicity of all new compounds were determined in transiently transfected PC-3 cells (Table 1–Table 5).[20] The data in the tables is intended to illustrate both potency and efficacy. This was done due to the observation that some compounds had equivalent potencies (IC_{50}s) against SRE.L, yet differed in their maximal responses (efficacies). There are a number of possible explanations for this, including differences in passive permeability into the cells, efflux out of the cells, or even the complement of Rho-pathway targets impacted. To optimize the likelihood for eventual *in vivo* activity, we elected to consider both potency and efficacy vs SRE.L in our structure-activity relationship (SAR) analysis. Effects against pRL-TK and WST-1 at high and low concentrations are included as an approximate indicator of selectivity. IC_{50}s often could not be calculated from the generally weaker dose response data against these selectivity targets, and therefore are not included.

Table 1 summarizes the impact of changes on the tether between the two carboxamides of compound **1**. Removing the methyl group (**5a**) had little effect on activity or selectivity. Replacement of the oxygen with carbon (**4a**) indeed removed acute cytotoxicity, even at high dose, and improved selectivity vs *Renilla*, but attenuated potency against SRE.L by over an order of magnitude. Decreasing or increasing the length of the carbon chain by one carbon (**4b** and **4c**) did not greatly impact the potency or efficacy relative to **4a**, but lengthening to four carbons (**4d**) resulted in a total loss of activity.

A brief survey of aromatic substitution is summarized in Table 2. Despite the diminished toxicity of **4a**, we elected to use the more potent unsubstituted aminoxyacetic acid template of **5a** to magnify any changes in activity. Moving the chloro group to the 3-position (**5b**) had no effect, but removing it altogether (**5c**) negatively affected both potency and efficacy. Removing one of the trifluoromethyl groups (**5d** and **5e**) was similarly detrimental to removing the chloro group, and removing both trifluoromethyl groups (**5f**) led to a complete loss of activity. Reversing the position of the two aromatic rings (**5g**) gave a compound with activity similar to **5a**. These limited data suggest that some degree of lipophilicity on the aromatic rings is crucial for activity, possibly to facilitate cell permeability. A more in-depth examination of aromatic substituent SAR, including whether electron deficiency is necessary, will be the subject of future work.

Table 3 summarizes our initial foray into modification of the secondary amides. N-methylation of the 4-chloroaniline amide (**4e**), intended to remove a hydrogen bond donor and improve cell permeability, resulted in a dramatic loss in activity. Replacement of one of the anilides with a benzylamide (**4f**) also was detrimental. Reducing the amides to the corresponding amines was considerably more successful. Both monoamines **8** and **11**, as well as diamine **12**, exhibited improved potency and efficacy against Rho-dependent gene expression. *Of particular interest was monoamine **8**, which had potency approaching that of the aminoxyacetic acid template **5a**, retained the moderate selectivity of **4a** vs non-specific gene expression, and showed very little cytotoxicity compared to the other monoamine and the diamine, even at high concentrations*. The other two amines exhibited unacceptable levels of cytotoxicity.

Conformational restriction of the flexible bis(amide) tether was explored as a way to potentially improve both potency and selectivity (Table 4). In several cases, improved potency vs the corresponding acyclic analog was observed (e.g. **4g** vs **4a**, **4p** vs **4e**), but the goal of improving selectivity vs non-specific gene expression was not clearly achieved with any of the restricted analogs. Among a series of closely related five- and six-membered ring analogs (**4g – 4j**), it is interesting to note that a "meta"-like disposition of the two aromatic rings (**4g**, **4j**) was favored over "para" or "ortho" in closely related analogs (**4h**, **4i**). This pattern is dramatically reflected in the series of analogs constrained by a central aromatic ring (**4l – 4n**), wherein only the meta analog **4m** is active. The inactivity of the vicinal substituted analog **4o** and an analog with a "vicinal-like" disposition of the amides (**19**) is also consistent with this pattern. Compound **20**, a restricted analog of monoamine **8**, was inferior to the acyclic analog with regard to both potency and efficacy, perhaps another example of the disadvantageous arrangement of the aromatic rings in a "para"-like orientation. Finally, reversal of the aromatic rings (**4q** vs **4h**) led to a significant loss in selectivity at high concentration vs *Renilla* and cytotoxicity.

Table 5 presents data for analogs incorporating potential bioisosteric replacements for one of the amides. Three of these compounds (**13**, **14** and **23**) exhibited improved potency vs the bis (amide) **4a**, but selectivity vs *Renilla* and/or cytotoxicity suffered. Triazoles **29** and **31** were completely inactive, perhaps suggesting a lack of permeability into the cells.

In our original publication, we showed that **1** selectively inhibited spontaneous PC-3 prostate cancer cell invasion through a Matrigel matrix, but not the $G\alpha_i$-dependent LPA-stimulated SKOV-3 ovarian cancer cell invasion, *in vitro*.[9] Therefore, we tested several of our analogs for their ability to inhibit PC-3 prostate cancer cell invasion with better selectivity for invasion versus toxicity (as measured by metabolism of WST-1) in comparison to **1**. Data for selected compounds is presented in Table 6[21]. Overall, a fairly consistent correlation was observed between inhibition of invasion and inhibition of SRE.L in PC-3 cells. For example, conformationally restricted analogs **4g – 4i**, which all possessed roughly equivalent efficacies against SRE.L at 10 and 100 µM, were similarly active in the Matrigel assay. Compound **4g**, however, was somewhat less toxic at the higher concentration, exhibiting an efficacy:toxicity profile at 100 µM that is superior to that of the original lead **1** at 10 µM. Also, a tight correlation between the selectivity for SRE.L:cytotoxicity and invasion:cytotoxicity can be seen in the series of amines **8**, **11** and **12**. Monoamine **8** had the most favorable ratio of efficacy to cytotoxicity in the transfected cell SRE-Luciferase studies, and this is reflected in the data in Table 6. This compound in fact inhibits invasion at 10 µM to an extent approaching that of the lead **1**, with no observable toxicity. At 100 µM, nearly complete inhibition of invasion was achieved with a lesser degree of toxicity than that induced by **1** at 10 µM. Monoamine **11** and diamine **12**, on the other hand, were much less selective for efficacy vs toxicity in the transfected cells (Table 3), and that is reflected in the data in Table 6 at the higher concentration.

Correlation graphs between the average inhibition of the PC-3 Matrigel invasion assay versus the average inhibition of the $G\alpha_{12}$QL-stimulated SRE.L-luciferase expression in PC-3 cells at 10 µM and 100 µM are presented in Figure 1. A positive correlation can be seen at both concentrations, although there are a few outliers that strongly inhibit SRE.L without inhibiting invasion. Interestingly, there seems to be a threshold for inhibition of SRE.L (about 50%) that must be achieved before effects on invasion are observed.

In summary, an initial SAR survey of **1**, an inhibitor of Rho-mediated gene expression, was undertaken with the goal of improving selectivity and/or potency, while attenuating cytotoxicity. In addition to removing the obviously labile N-O bond, two strategies were applied: 1) replacement of the secondary carboxamides to improve cell permeability; and 2) conformational restriction to improve potency and/or selectivity. These approaches afforded compounds with improved biological profiles relative to the lead **1**, albeit at a cost of 5–10-

fold lower potencies. Of particular interest are nipecotic amide **4g** and monoamine **8**, each of which are capable of inhibiting $G\alpha_{12}$QL-stimulated SRE.L-luciferase expression with efficacy equal to that of **1**, but with significantly less attendant cytotoxicity. Furthermore, we have for the first time demonstrated within this series of compounds a clear correlation between inhibition of Rho-mediated gene expression and cell invasion in a Matrigel matrix model of metastasis.

Future work will be aimed at expanding the diversity of the aromatic rings using one or both of the improved templates of **4g** and **8**, as well as constructing affinity reagents for the identification of the molecular target(s) of this novel class of inhibitors of the Rho-signaling pathway.

Acknowledgments

Supported by NIH grants R01GM39561 (RRN) and F31CA113268-04 (CRE) and support from the UM Comprehensive Cancer Center and the Prostate Cancer SPORE (P50CA069568).

References and notes

1. Sawyer TK. Expert Opinion on Investigational Drugs 2004;13:1–19. [PubMed: 14680449]
2. Sahai E, Marshall C. J. Nat Cell Biol 2003;5:711–719.
3. van Golen KL, Wu ZF, Qiao XT, Bao LW, Merajver SD. Cancer Res 2000;60:5832–5838. [PubMed: 11059780]
4. Liu N, Zhang G, Bi F, Pan Y, Xue Y, Shi Y, Yao L, Zhao L, Zheng Y, Fan D. J Mol Med 2007;85:1149–1156. [PubMed: 17549441]
5. Cen B, Selvaraj A, Burgess RC, Hitzler JK, Ma Z, Morris SW, Prywes R. Mol Cell Biol 2003;23:6597–6608. [PubMed: 12944485]
6. Miralles F, Posern G, Zaromytidou AI, Treisman R. Cell 2003;113:329–342. [PubMed: 12732141]
7. Hakem A, Sanchez-Sweatman O, You-Ten A, Duncan G, Wakeham A, Khokha R, Mak TW. Genes Dev 2005;19:1974–1979. [PubMed: 16107613]
8. Medjkane S, Perez-Sanchez C, Gaggioli C, Sahai E, Treisman R. Nat Cell Biol 2009;11:257–268. [PubMed: 19198601]
9. Evelyn CR, Wade SM, Wang Q, Wu M, Iniguez-Lluhi JA, Merajver SD, Neubig RR. Molecular Cancer Therapeutics 2007;6:2249–2260. [PubMed: 17699722]
10. Lipinski CA, Lombardo F, Dominy BW, Feeney PJ. Advanced Drug Delivery Reviews 1997;23:3–25.
11. Burton PS, Conradi RA, Ho NF, Hilgers AR, Borchardt RT. J Pharm Sci 1996;85:1336–1340. [PubMed: 8961149]
12. Veber DF, Johnson SR, Cheng HY, Smith BR, Ward KW, Kopple KD. J Med Chem 2002;45:2615–2623. [PubMed: 12036371]
13. Lima LM, Barreiro E. J. Curr Med Chem 2005;12:23–49.
14. Mann, A.; LeChatlier, HL. Practice of Medicinal Chemistry. London: Elsevier; 2003. p. 233-250.
15. Orelli LR, Garcia MB, Niemevz F, Perillo IA. Synthetic Communications 1999;29:1819–1833.
16. Klapars A, Huang XH, Buchwald SL. Journal of the American Chemical Society 2002;124:7421–7428. [PubMed: 12071751]
17. Liu A, Liu A. Journal of Agricultural and Food Chemistry 2008;56:6562. [PubMed: 18598043]
18. Tellitu I, Urrejola A, Serna S, Moreno I, Herrero MT, Dominguez E, SanMartin R, Correa A. European Journal of Organic Chemistry 2007:437–444.
19. Rostovtsev VV, Green LG, Fokin VV, Sharpless KB. Angewandte Chemie-International Edition 2002;41:2596.
20. PC-3 cells were seeded into 96-well plates at a cell density of 4×10^4 cells per well 24 hours prior to transient transfection with a Gα12Q231L activator expression plasmid along with both the SRE.L luciferase and pRL-TK *Renilla* luciferase reporter plasmids. The DNA plasmids were transfected

using the lipid-based LipofectAMINE 2000 (Invitrogen) transfection reagent at a concentration of 1 μL per μg of DNA in antibiotic-free, Opti-MEM I medium. The total amount of DNA was kept constant by inclusion of the appropriate amount of the pcDNA3.1-zeo plasmid. Six hours after transfection, the transfection mixture was removed and cells were serum-starved overnight in DMEM medium containing 0.5% FBS and 1% penicillin-streptomycin. Firefly and *Renilla* luciferase activities were determined 19 hours later using the dual-luciferase assay kit (Promega) according to the manufacturer's instructions. Just before cell lysis, the viability of the cells was measured using a WST-1 cell proliferation reagent. Data are expressed as IC_{50} or percentage of inhibition (DMSO alone = 0%) in Table 1 – Table 5. Individual experiments were run in triplicate, and the values in the tables are the mean of at least three separate experiments. Because of the large degree of variability inherent in transient transfection assays, standard error measurements have not been included.

21. Compounds were tested as follows: PC-3 cells (2×10^5) were transferred to 24-well Matrigel inserts in low-serum DMEM medium (0.5% FBS) with DMSO or chemical compounds in the upper chamber. Low-serum DMEM medium (0.5% FBS) was added to the lower well and the invasion chambers were incubated at 37 °C in 5% CO_2 for 24 hours. Inserts were fixed in methanol for 10 min and then stained for 60 min with 0.5% crystal violet in 20% methanol. After wiping the top surface of the filter with cotton swabs to remove non-invaded cells, the inserts were allowed to dry overnight. Inserts were incubated in 20% acetic acid on a plate shaker for 15 min to extract the crystal violet stain. The number of invaded cells was quantitated by measuring the absorbance of the extracted crystal violet stain at a wavelength of 595 nm with the Victor[2] plate reader.

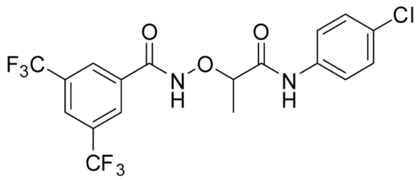

1 (CCG-1423)

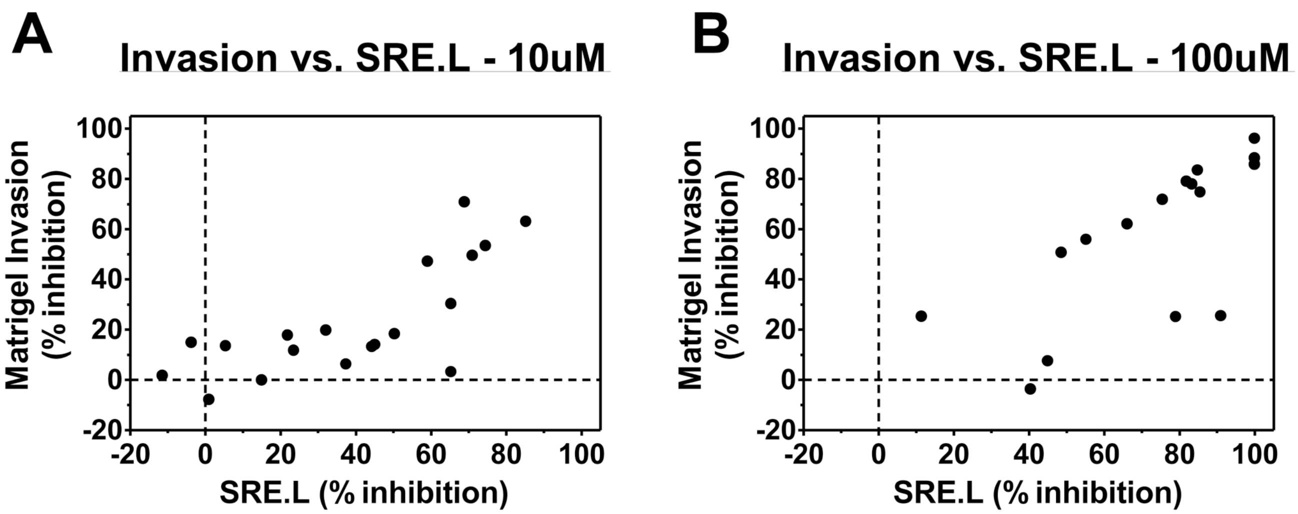

Figure 1.
Correlation of Matrigel invasion and Gα_{12}QL-stimulated SRE.L-luciferase expression inhibition in PC-3 cells. The data represent the average of experiments performed 3 separate times for an n = 3 in duplicate and triplicate, respectively.

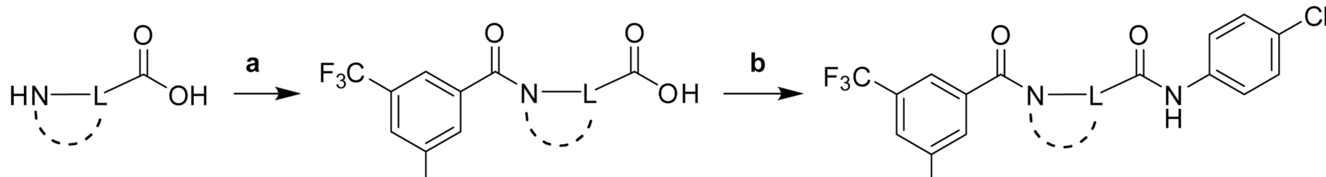

Scheme 1.

Reagents and conditions: (a) 3,5-bis(CF_3)PhCOCl, aq NaOH, RT, overnight; or 3,5-bis(CF_3) PhCOCl, triethylamine (TEA), CH_2Cl_2 ; (b) 4-ClPhNH_2, EDC, HOBt, DIPEA, THF, RT, overnight.

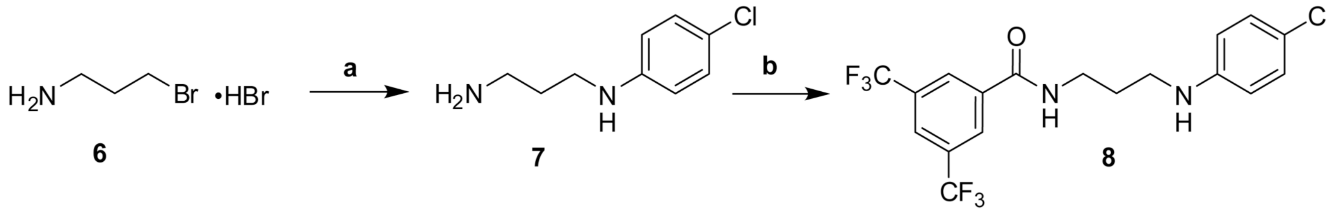

Scheme 2.
Reagents and conditions: (a) 4-ClPhNH_2, PhMe, reflux, 45 min, 28%; (b) 3,5-bis(CF_3)PhCOOH, HOBt, EDC, DIPEA, THF, RT, overnight, 65%.

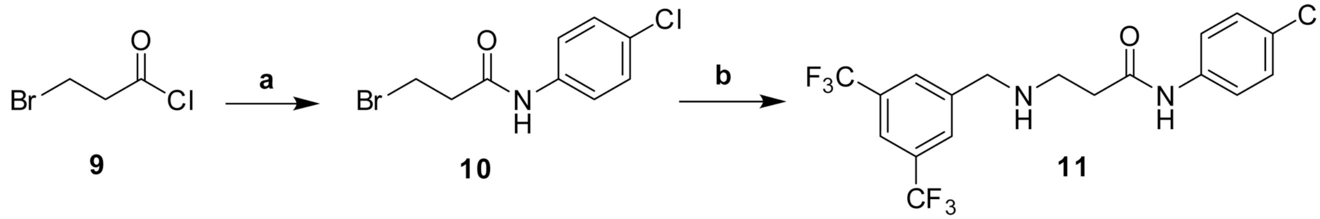

9 10 11

Scheme 3.
Reagents and conditions: (a) 4-ClPhNH_2, MeCN, reflux, 3 h, 94%; (b) 3,5-bis(CF_3)PhCH_2NH_2, MeCN, reflux, 7 h, 99%.

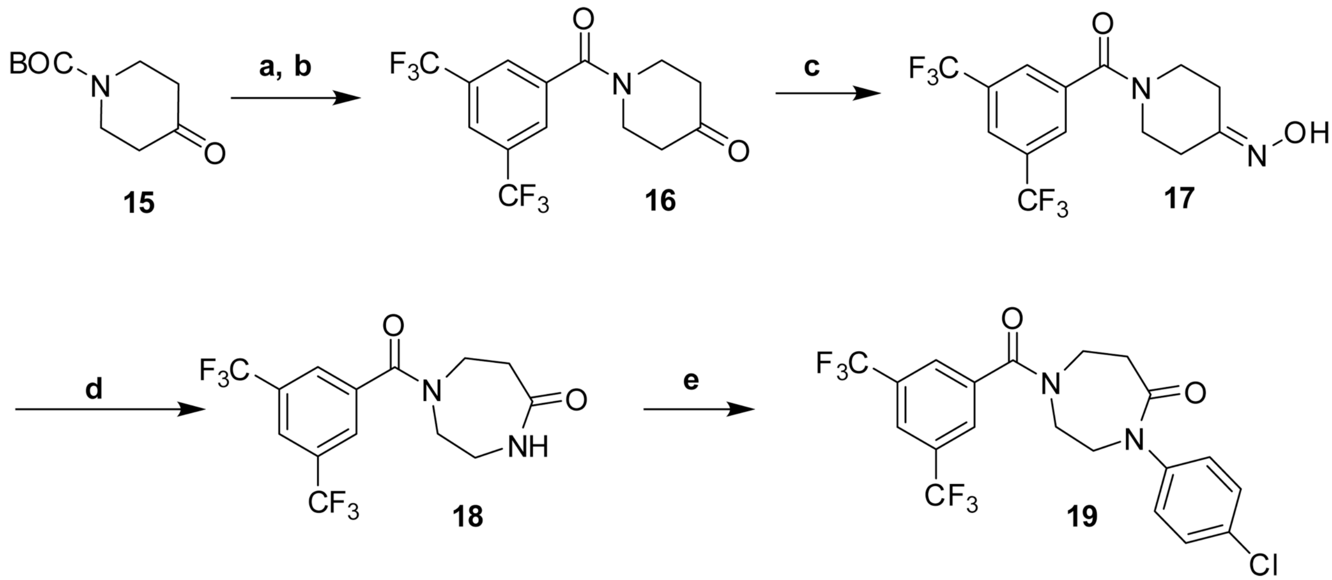

Scheme 4.

Reagents and conditions: (a) TFA, CH_2Cl_2, 0°C to RT, 3h, quant.; (b) 3,5-bis(CF_3)PhCOCl, aq NaOH, RT, overnight, 74%; (c) NH_2OH•HCl, pyridine, 3Å sieves, RT, overnight, 72%; (d) Na_2CO_3, p-TsCl, acetone, RT, 3 h, 66%; (e) 4-I-PhCl, $MeNHCH_2CH_2NHMe$, CuI, Cs_2CO_3, dioxane, 100 °C, 24 h, 48%.

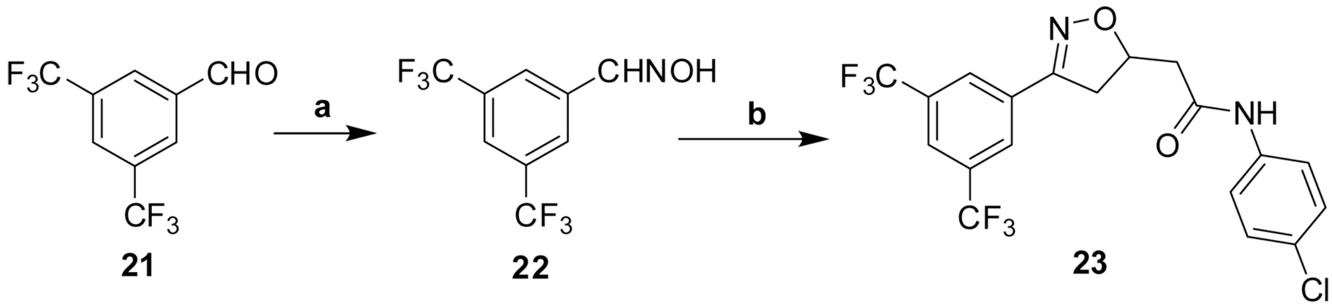

21 22 23

Scheme 5.

Reagents and conditions: (a) $HONH_2$•HCl, MeOH, reflux, 5 h, 48%; (b) N-(4-chlorophenyl) but-3-enamide, NaOCl, CH_2Cl_2, 0°C to RT, 24 h, 99%.

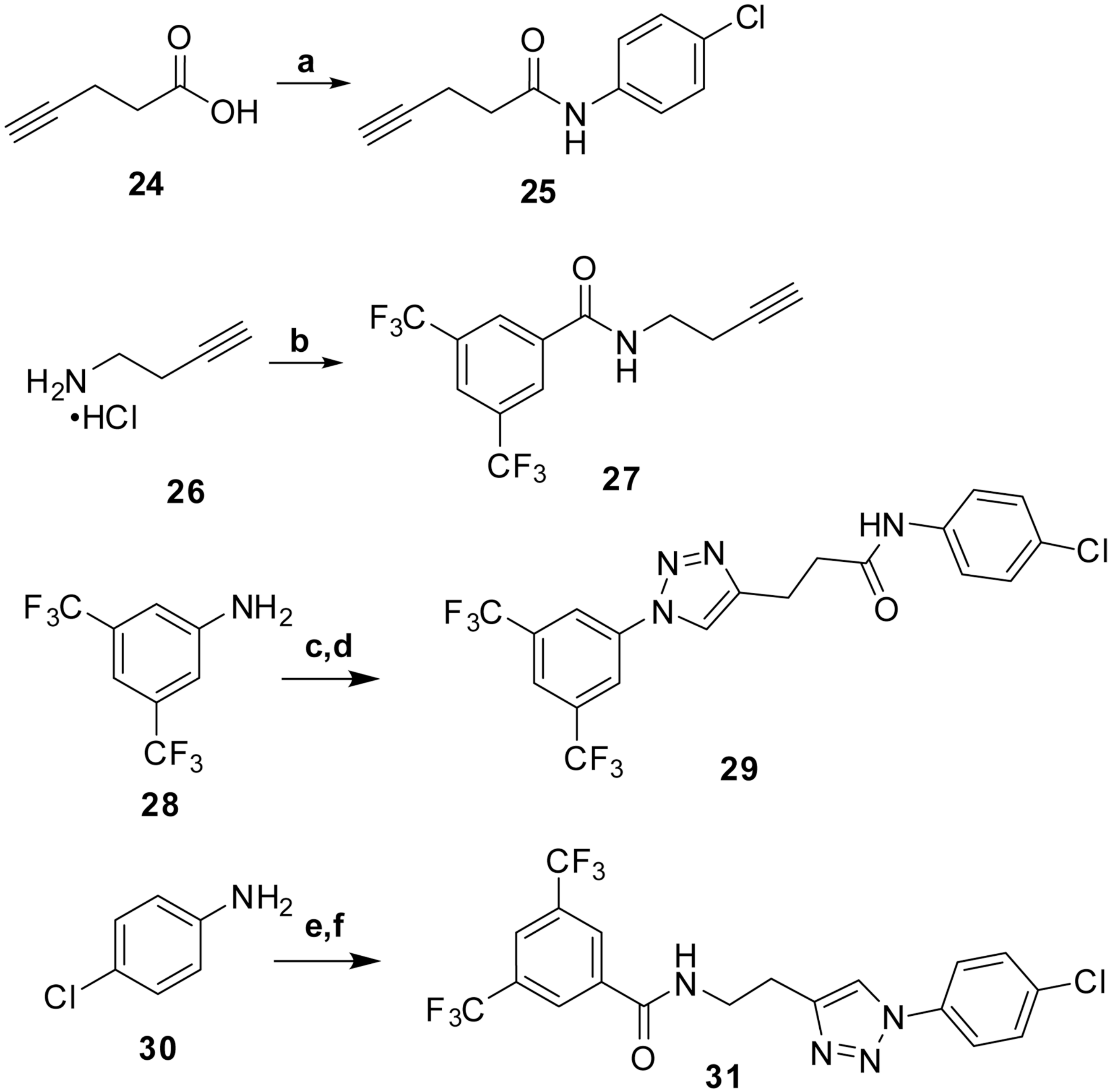

Scheme 6.

Reagents and conditions: (a) 4-ClPhNH$_2$, HOBt, EDC, DIPEA, THF, RT, overnight, 87%; (b) 3,5-bis(CF$_3$)COCl, TEA, CH$_2$Cl$_2$, RT, overnight, 97%; (c) i. TFA, −10 °C, NaNO$_2$; ii. NaN$_3$, −10 °C to RT, 2 h, 63%; (d) **25**, CuSO$_4$•5H$_2$O, L-Ascorbic acid, H$_2$O/tBuOH, 1:1, RT, overnight, 19%; (e) i. 6M HCl, 0 °C, NaNO$_2$; ii. NaN$_3$, 0 °C, 15 min., 56%; (f) **27**, CuSO$_4$•5H$_2$O, L-Ascorbic acid, H$_2$O/tBuOH, 1:1, RT, 48 h, 10%.

Table 1

Effects of tether length and composition on transcription and cytotoxicity in transfected PC-3 cells[a]

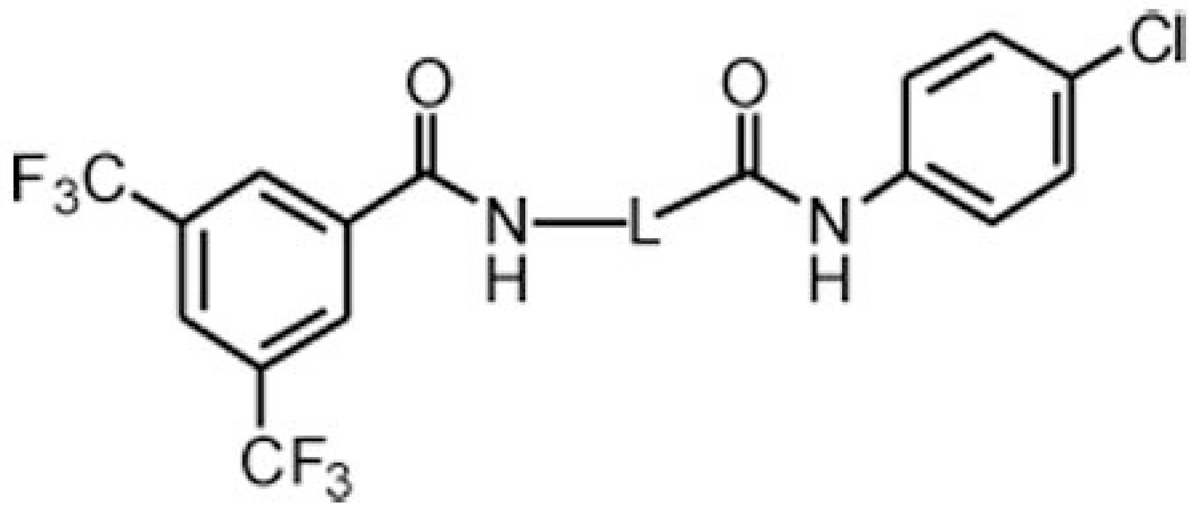

Cmpd	L	IC_{50} SRE.L[b] (μ M)	% inh SRE.L[b] (10, 100 μM)	% inh pRL-TK[c] (10, 100 μM)	% inh WST-1[d] (10, 100 μM)
1	$-OCH(CH_3)-$	1.5	74, ND	48, ND	44, ND
5a	$-OCH_2-$	4.7	71, 100	53, 89	42, 91
4a	$-CH_2CH_2-$	38	38, 64	0, 22	0, 10
4b	$-CH_2-$	33	45, 85	15, 25	0, 30
4c	$-CH_2CH_2CH_2-$	21	37, 79	5, 42	0, 12
4d	$-CH_2CH_2CH_2CH_2-$	>100			

[a]For assay descriptions, see Ref [20]. All values are mean of ≥ 3 experiments, each run in triplicate.

[b]Inhibition of Rho-pathway selective serum response element-luciferase reporter.

[c]Inhibition of control pRL-thymidine kinase *Renilla* luciferase reporter.

[d]Inhibition of mitochondrial metabolism of WST-1.

Table 2

Effects of aromatic substitution on transcription and cytotoxicity in transfected PC-3 cells[a]

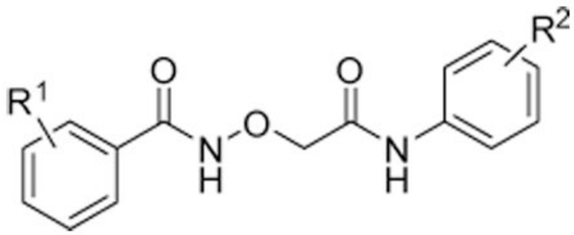

Cmpd	R^1	R^2	IC_{50} SRE.L (μM)	% inh SRE.L (10, 100 μM)	% inh pRL-TK (10, 100 μM)	% inh WST-1 (10, 100 μM)
5a	3,5-bis(CF_3)	4-Cl	4.7	71, 100	53, 89	42, 91
5b	3,5-bis(CF_3)	3-Cl	5.9	65, 100	51, 89	49, 97
5c	3,5-bis(CF_3)	4-H	36	13, 65	33, 59	0, 37
5d	3-CF_3	4-Cl	27	25, 86	5, 19	0, 58
5e	4-CF_3	4-Cl	29	26, 91	6, 0	0, 56
5f	4-H	4-Cl	>100			
5g	4-Cl	3,5-bis(CF_3)	8.6	58, 100	19, 87	11, 96

[a] Assays defined in Table 1.

Table 3

Effects of amide modifications on transcription and cytotoxicity in transfected PC-3 cells[a]

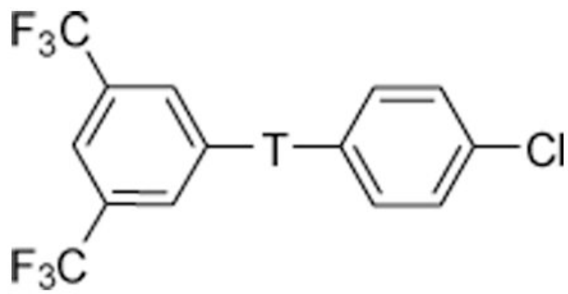

Cmpd	T	IC_{50}SRE.L (μM)	% inh SRE.L (10, 100 μM)	% inh pRL-TK (10, 100 μM)	% inh WST-1 (10, 100 μM)
4a	$-CONHCH_2CH_2CONH-$	38	38, 64	0, 22	0, 10
4e	$-CONHCH_2CH_2CON(\mathbf{Me})-$	>100			
4f	$-CONHCH_2CH_2CONH\mathbf{CH_2}$	>100			
8	$-CONHCH_2CH_2\mathbf{CH_2}NH-$	5.1	70, 80	37, 35	0, 11
11	$\mathbf{-CH_2}NHCH_2CH_2CONH-$	8.1	64, 100	12, 91	0, 92
12	$\mathbf{-CH_2}NHCH_2CH_2\mathbf{CH_2}NH-$	9.1	65, 100	6, 90	0, 89

[a] Assays defined in Table 1.

NIH-PA Author Manuscript
NIH-PA Author Manuscript

Table 4

Effects of conformational restriction on transcription and cytotoxicity in transfected PC-3 cells[a]

Cmpd	Structure	IC_{50} SRE.L (μM)	% inh SRE.L (10, 100 μM)	% inh pRL-TK (10, 100 μM)	% inh WST-1 (10, 100 μM)
4a	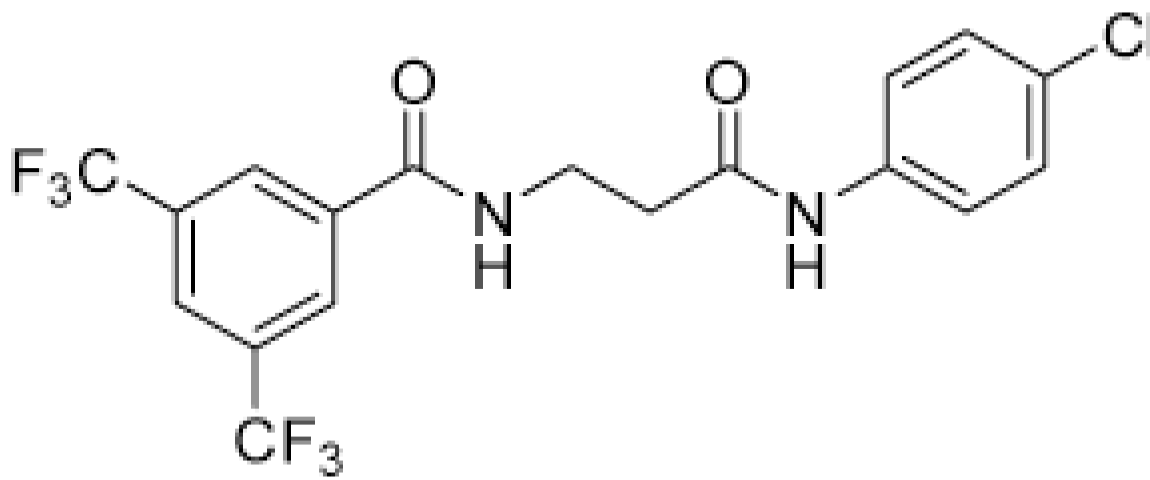	38	38, 64	0, 22	0, 10
4g	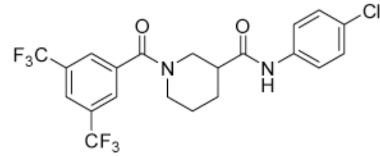	9.8	37, 78	19, 34	0, 14
4h	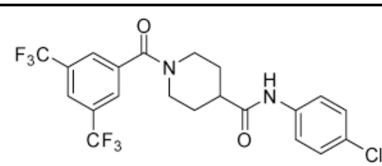	16	17, 87	0, 17	0, 39

Cmpd	Structure	IC_{50} SRE.L (μM)	% inh SRE.L (10, 100 μM)	% inh pRL-TK (10, 100 μM)	% inh WST-1 (10, 100 μM)
4i	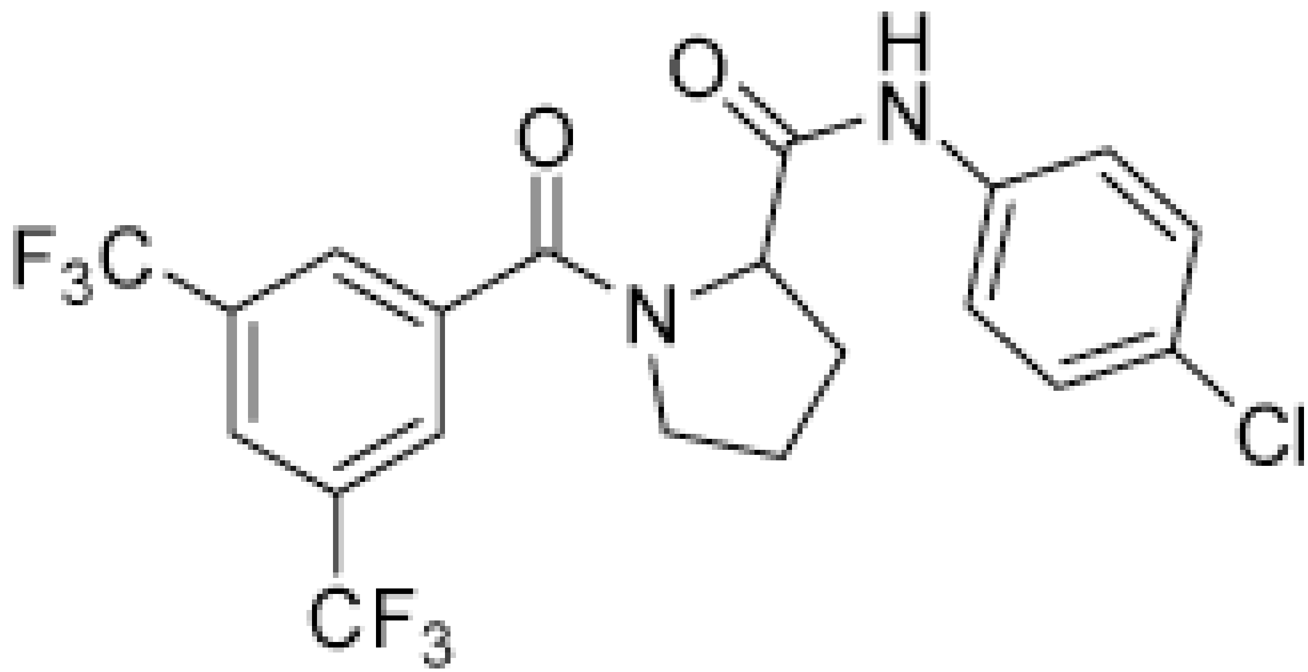	69	23, 83	12, 27	0, 22

Cmpd	Structure	IC_{50} SRE.L (μM)	% inh SRE.L (10, 100 μM)	% inh pRL-TK (10, 100 μM)	% inh WST-1 (10, 100 μM)
4j	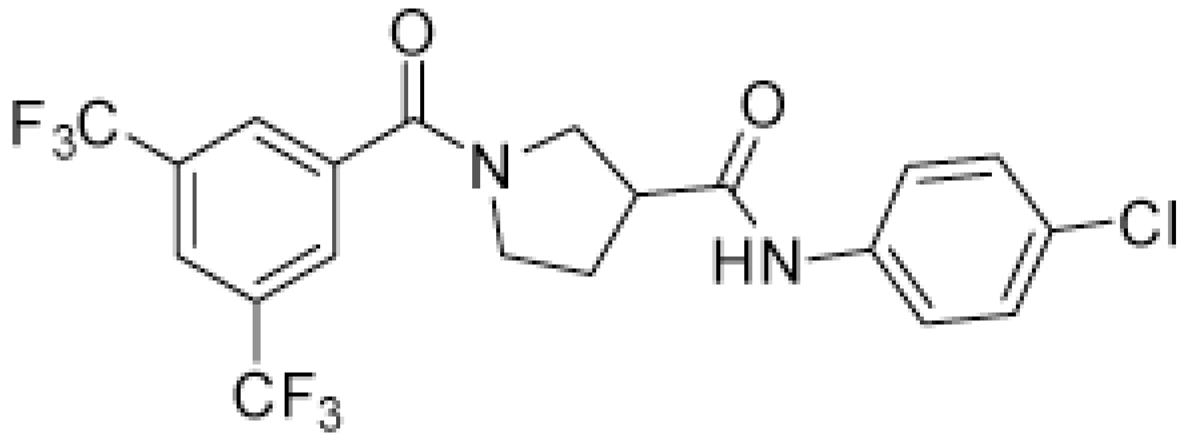	16.3	30, 100	8, 78	0, 67
4k	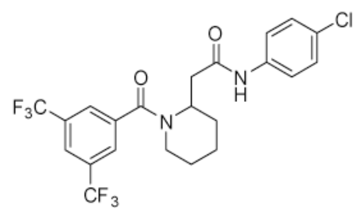	9.5	33, 86	0, 62	0, 14

Cmpd	Structure	IC_{50} SRE.L (μM)	% inh SRE.L (10, 100 μM)	% inh pRL-TK (10, 100 μM)	% inh WST-1 (10, 100 μM)
4l	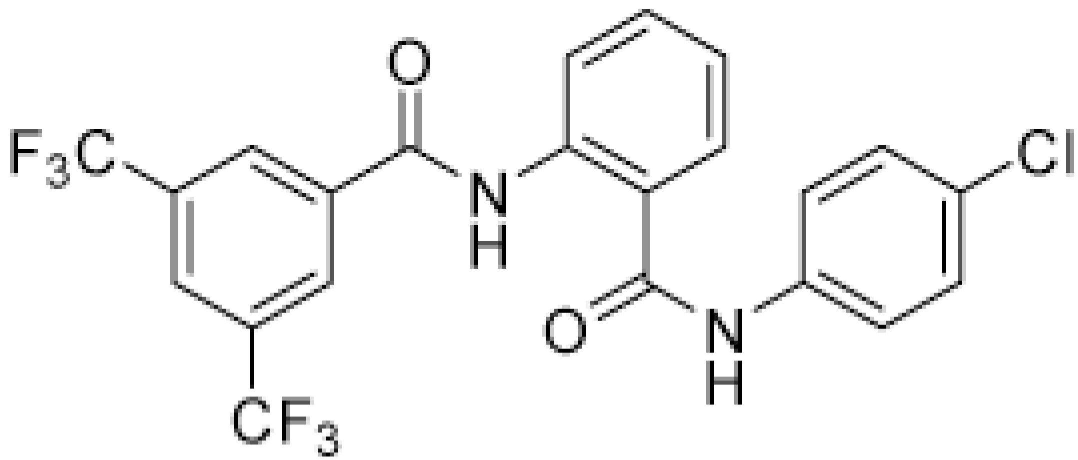	>100			
4m	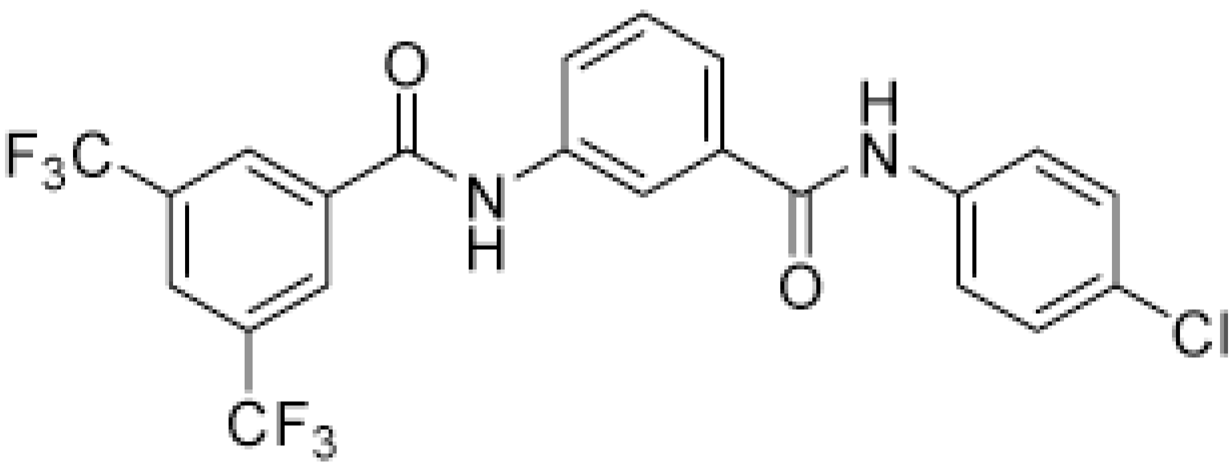	1.7	79, ND	0, ND	38, ND

Cmpd	Structure	IC_{50} SRE.L (μM)	% inh SRE.L (10, 100 μM)	% inh pRL-TK (10, 100 μM)	% inh WST-1 (10, 100 μM)
4n	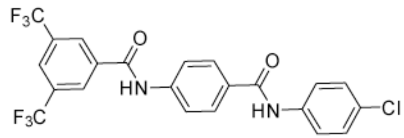	>100			
4o	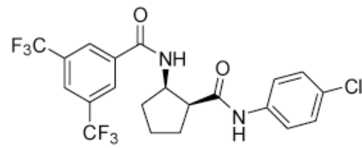	>100			
4p	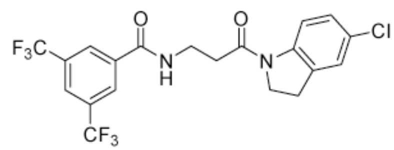	13	15, 40	0, 1	0, 0

Cmpd	Structure	IC_{50} SRE.L (μM)	% inh SRE.L (10, 100 μM)	% inh pRL-TK (10, 100 μM)	% inh WST-1 (10, 100 μM)
4q	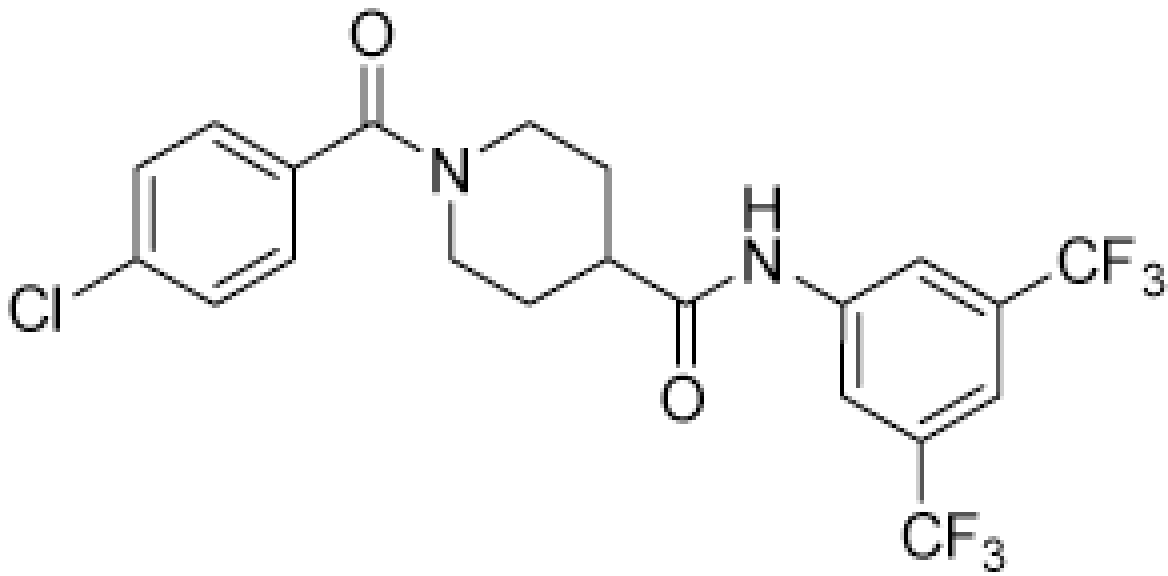	10	51, 100	30, 91	10, 88
19	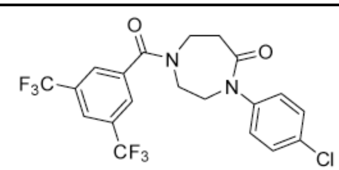	>100			
20	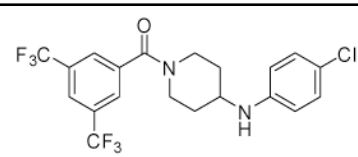	10.8	19, 54	0, 20	0, 0

[a]Assays defined in Table 1. ND: not determined.

NIH-PA Author Manuscript
NIH-PA Author Manuscript

Table 5

Effects of amide replacement on transcription and cytotoxicity in transfected PC-3 cells[a]

Cmpd	Structure	IC_{50} SRE.L (μM)[a]	% inh SRE.L (10, 100 μM)[b]	% inh pRL-TK (10, 100 μM)[b]	% inh WST-1 (10, 100 μM)[b]
4a	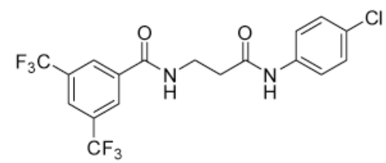	38	38, 64	0, 22	0, 10
13	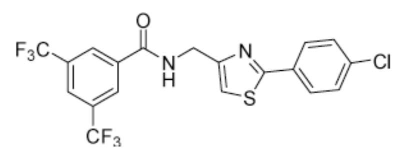	4.1	50, 45	39, 38	0, 0
14	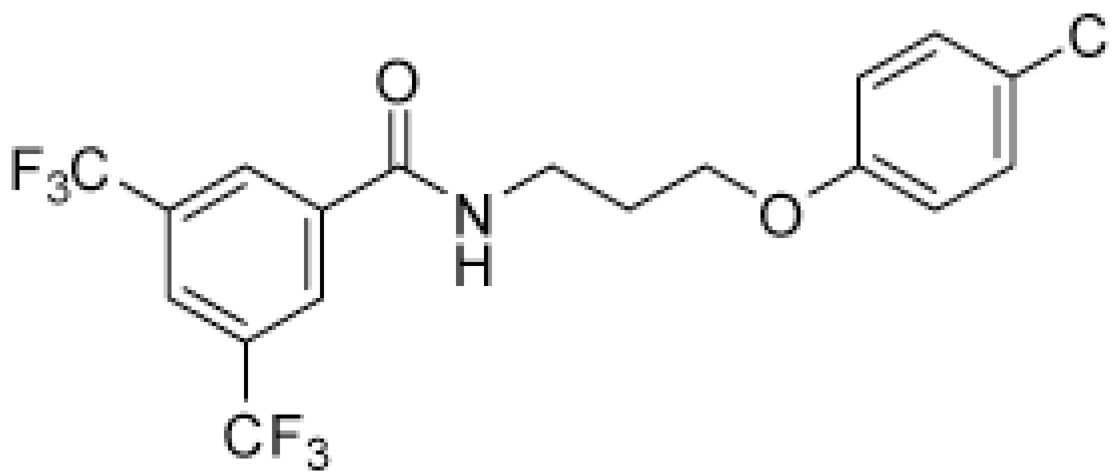	8.9	55, 86	28, 65	0, 38

Cmpd	Structure	IC_{50} SRE.L (μM)[a]	% inh SRE.L (10, 100 μM)[b]	% inh pRL-TK (10, 100 μM)[b]	% inh WST-1 (10, 100 μM)[b]
23	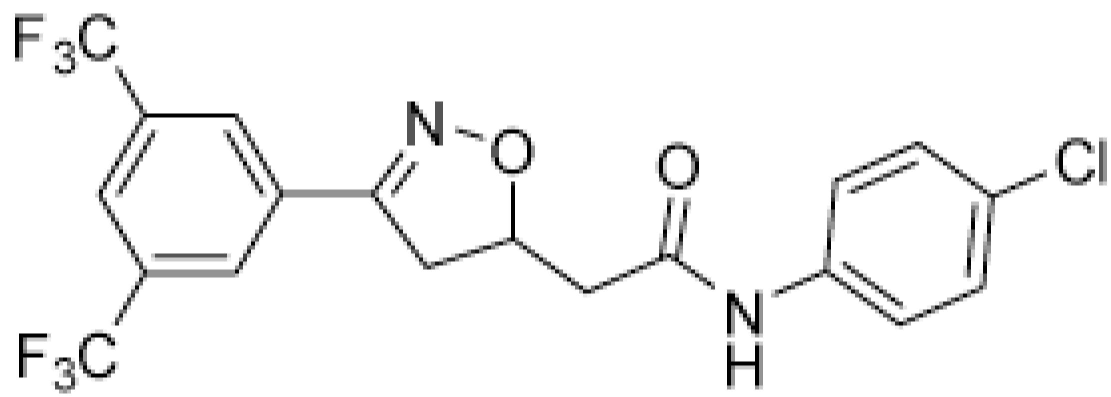	4.2	70, 84	51, 60	0, 38
29	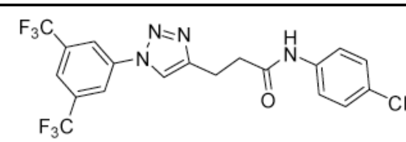	>100			
31	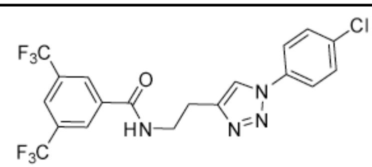	>100			

[a]Assays defined in Table 1.

Table 6

Effects of new analogs on cell invasion and cytotoxicity[a]

Cmpd	% inh invasion[b] (10 μM)	% inh WST-1[c] (10 μM)	% inh invasion[b] (100 μM)	% inh WST-1[c] (100 μM)
1	71	54		
4a	13	0	62	28
4b	14	0	75	38
4c	6	0	31	1
4d	15	0	25	1
4g	20	0	72	23
4h	14	0	79	36
4i	12	0	78	44
4m	63	31	86	70
4n	2	0	0	1
4p	0	0	0	0
5a	50	14	88	78
8	54	0	84	27
11	47	0	96	95
12	30	0	86	97
13	18	0	8	0
14	3	0	26	0
20	18	0	56	0

[a]For assay descriptions, see Ref [21].

[b]Inhibition of invasion by cultured PC-3 cells into a Matrigel matrix.

[c]Inhibition of mitochondrial metabolism of WST-1.